A Mechatronic Lock-In Amplifier: Integrating Demodulation in Sensor Electronics for Measuring Mechanical Oscillations

Mathias Poik, Dominik Kohl, Mario Mayr, Christoph Kerschner, Georg Schitter *Senior Member, IEEE*
Automation and Control Institute (ACIN), Technische Universität Wien
Vienna, Austria
poik@acin.tuwien.ac.at

***Abstract*—The demodulation of mechanical oscillations is essential for the operation of micro -and nanometer scale transducer systems, such as resonant MEMS mirrors and cantilever-based sensors. The use of external demodulators, such as lock-in amplifiers and spectrum analyzers is not always desired due to their large size, complexity and cost. The method presented in this paper enables a simplified demodulation of the oscillation of mechanical oscillators with integrated deflection sensors. By configuring two deflection sensors in separate bridge circuits, which are supplied with in-phase and quadrature sinusoidal signals, the amplitude and phase of the mechanical oscillation can directly be measured without additional demodulation. The method is implemented and experimentally verified by demodulating the oscillation of a self-sensing Atomic Force Microscopy cantilever with integrated piezoresistive elements.**

***Index Terms*—Demodulation, Lock-In Amplifier, Resonant sensor, Cantilever, AFM**

I. Introduction

Mechanical oscillators are crucial components in micro -and nanometer scale transducer applications. For instance, resonant MEMS mirrors enable high speed laser beam steering, which is essential for modern optical scanning systems, such as Light Detection and Ranging (LIDAR) [1], photoacoustic imaging [2] and optical endoscopy [3]. Micro-machined cantilevers are used in a variety of sensor applications, such as biosensing [4], chemical and environmental detection [5], as well as the local measurement of surface properties by Atomic Force Microscopy (AFM) [6].

The ability to measure and control the laser spot position typically defines the accuracy of optical scanning systems. Resonant MEMS mirrors used for beam steering therefore require an accurate measurement of their oscillation amplitude and phase [7]. On the other hand, resonant cantilever-based sensors detect the variation of the resonance frequency caused by changes of the cantilever mass or stiffness due to its interaction with the environment [8], [9]. To this end, the cantilever is typically excited by an external stimulus, provided by acoustic, thermal or electrical actuators [10], and the resonance frequency is measured by analyzing the frequency spectrum of the resulting oscillation [11]. To enhance the selectivity of the measurement, i.e. to reduce unwanted influences such as temperature or humidity, the resonance frequency can be tracked by adjusting the excitation frequency in a feedback loop. To this end, the oscillation phase is measured and the excitation frequency is controlled such that the phase difference between excitation signal and oscillation is kept constant [12]. Similarly, in various dynamic AFM measurement modes the oscillation amplitude and/or phase are typically measured using lock-in amplifiers and controlled in a feedback loop [13]–[15]. For instance, in intermittent contact mode the amplitude is kept constant and the sample position is adjusted to determine the surface topography, while the phase can be simultaneously recorded to determine additional mechanical properties of the surface [16]. The measurement of amplitude and phase, which requires the detection and demodulation of the mechanical oscillation, is therefore a crucial part of micro -and nanometer scale transducer systems.

For the detection of the mechanical oscillation, which can range from the sub-nm to the μm range, different methods are applied [17]. The optical lever method is most commonly applied for measuring the oscillation of cantilever-based sensors [18]. It enables a highly sensitive and reliable measurement of cantilever deflections down to a few angstroms. A disadvantage of the method is that laser and detector are usually mounted outside of the measurement chamber containing cantilever and its surrounding fluid or gas, which requires the laser to pass through several boundary interfaces. In the case of resonant mirrors, the optical path is needed by the laser scanning application. Additionally, the measurement method requires a cumbersome laser alignment process and the entire measurement system is bulky and not suited for mass production. Piezoresistive and capacitive detection schemes convert the deflection to a change of the electrical impedance, which is detected by an electrical read-out system [19], [20]. A disadvantage of these detection schemes is the typically lower sensitivity with respect to the optical detection [21]. An advantage is the possibility to miniaturize and integrate the piezoresistive or capacitive elements directly on the mechanical oscillator. It therefore enables a compact detection system which can be mass-produced at low cost, and enables an easy extension to parallel probing systems [22] or cantilever arrays [23].

The detection methods provide an electrical signal proportional to the harmonic oscillator motion, which has to be demodulated to determine the oscillation amplitude and phase. Wide-band demodulation techniques, such as peak-hold

Pre-print version of the article: M. Poik, D. Kohl, M. Mayr, C. Kerschner and G. Schitter, "A Mechatronic Lock-In Amplifier: Integrating Demodulation in Sensor Electronics for Measuring Mechanical Oscillations", *IEEE Transactions on Instrumentation and Measurement*, vol. 70, 2020. DOI: 10.1109/TIM.2020.3047208

detectors [24] or RMS-to-DC converters [25], enable a simple amplitude measurement with low implementation complexity. However, these methods are sensitive to measurement noise at other frequency components, and do not enable a phase measurement. Due to their selectivity, narrow-band demodulation methods, such as lock-in amplifiers [1], [26], [27], impedance analyzers [28] and spectrum analyzers [11] are therefore most widely used for the demodulation. However, the high resonance frequencies in the mentioned transducer applications, which are ranging from several kHz for MEMS mirrors to tens of MHz for cantilever-based sensors, lead to a high implementation complexity of such demodulators. Today's lock-in amplifiers are implemented on digital signal processors requiring sampling rates which are 10 to 100 times higher than the oscillation frequencies [29]. Additionally, fast ADCs with 14 to 16-bit resolution are typically needed for a high resolution measurement of the oscillation. The size, cost and complexity of the demodulator can therefore by far exceed those of the micro-machined oscillator itself, which presents a severe limitation of the overall transducer or sensor system.

The contribution of this paper is an efficient method for the demodulation of mechanical oscillations integrated with the sensor electronics, which can eliminate the need for bulky and costly external demodulation techniques in many applications. The presented method enables a simultaneous and independent measurement of amplitude and phase of mechanical oscillations by integrating the lock-in technique in the sensor electronics. This paper is an extension of our previous work [30], which only allowed the measurement of the oscillation amplitude under the condition that the phase remains constant. The proposed method is demonstrated by demodulating the oscillation of a self-sensing AFM cantilever. The paper is organized as follows. Section II presents a system description and a review of the conventional demodulation by a lock-in amplifier. The proposed method is described in Section III. The experimental implementation and the measurement results are presented in Section IV and Section V, respectively. Section VI concludes the paper.

II. System Description

In this work, the oscillation of a self-sensing AFM cantilever (PRSA-L300-F50-Si-PCB, SCLSensortech, Vienna, Austria) with integrated piezoresistive elements is measured to demonstrate the proposed demodulation method. The first mechanical resonance frequency of the cantilever equals $\omega_0 = 2\pi \cdot 92.3\,\mathrm{kHz}$. As illustrated in Figure 1 (left), the piezoresistive elements are placed at the base of the cantilever and connected in a half bridge circuit to detect the small changes of their resistance due the cantilever deflection. As shown in the microscope image in Figure 2, the passive resistors in the bridge circuit are integrated on the chip of the AFM cantilever, such that the bridge is thermally compensated. All resistors have an identical nominal resistance (without cantilever deflection) of $R = 1.07\,\mathrm{k\Omega}$. The chip is vibrated by a piezoelectric actuator (PhysikInstrumente, Karlsruhe, Deutschland) at the first resonance frequency ω_0 of the cantilever. For a cantilever

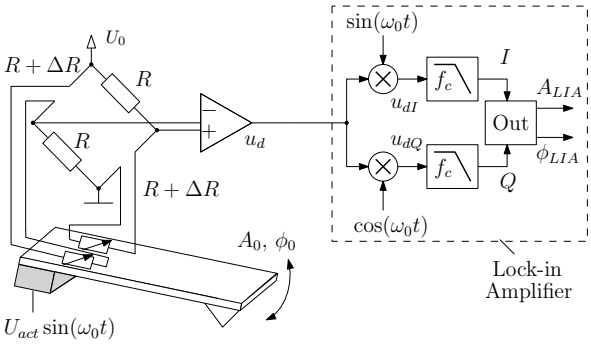

Fig. 1: Conventional demodulation of the cantilever oscillation. The piezoresistive element is connected in a DC bridge circuit and the resulting differential voltage is applied to a lock-in amplifier.

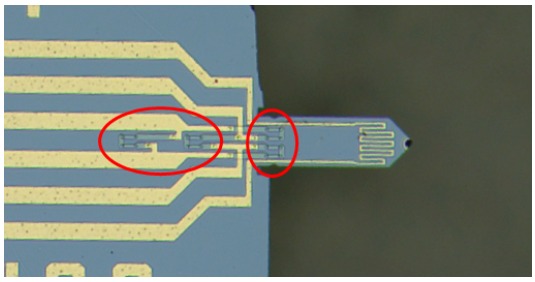

Fig. 2: Microscope image of a self-sensing AFM cantilever with integrated piezoresistive elements at its base (right circle), and two additional piezoresistive elements on the chip (left circle). The piezoresistive elements are connected in a half bridge circuit.

oscillation at ω_0, the resulting variation ΔR of the resistance can be expressed as

$$\Delta R(t) = K A_0 \sin(\omega_0 t + \phi_0)\,, \tag{1}$$

where A_0 and ϕ_0 denote oscillation amplitude and phase, and K denotes the piezoresistive sensitivity [31]. The output of the bridge circuit is connected to an instrumentation amplifier. Assuming $\Delta R \ll R$, which is typically valid for the small deflections of the cantilever, the voltage u_d at the output of the instrumentation amplifier equals

$$u_d(t) \approx \frac{U_0 K}{2R} A_0 \sin(\omega_0 t + \phi_0)\,, \tag{2}$$

with the supply voltage U_0.

In an AFM application the interaction forces between the tip and the investigated surface lead to a modulation of the cantilever oscillation and therefore to a time-dependent amplitude A_0 and/or phase ϕ_0. In order to determine A_0 and ϕ_0, the voltage u_d has to be demodulated.

A. Conventional Demodulation by Lock-In Amplifier

In this section, the working principle of a lock-in amplifier is reviewed as conventional method. The proposed demodulation method is presented in the following Section III.

Pre-print version of the article: M. Poik, D. Kohl, M. Mayr, C. Kerschner and G. Schitter, "A Mechatronic Lock-In Amplifier: Integrating Demodulation in Sensor Electronics for Measuring Mechanical Oscillations", *IEEE Transactions on Instrumentation and Measurement*, vol. 70, 2020. DOI: 10.1109/TIM.2020.3047208

Figure 1 (dashed box) shows the working principle of the demodulation by a lock-in amplifier. The instrumentation amplifier output voltage u_d (2) is multiplied by in-phase ($\sin(\omega_0 t)$) and quadrature ($\cos(\omega_0 t)$) sinusoidal signals. The resulting voltages u_{dI} and u_{dQ} after the multiplication

$$u_{dI}(t) = \frac{U_0 K}{4R} A_0 \left[\cos(\phi_0) - \cos(2\omega_0 t + \phi_0)\right] , \quad (3)$$

$$u_{dQ}(t) = \frac{U_0 K}{4R} A_0 \left[\sin(\phi_0) + \sin(2\omega_0 t + \phi_0)\right] \quad (4)$$

are applied to low-pass filters with a $-3\,\mathrm{dB}$ bandwidth of f_c to suppress the spectral components at $2\omega_0$ and obtain the in-phase and quadrature voltages I and Q:

$$I = \frac{U_0 K}{4R} A_0 \cos(\phi_0) , \quad (5)$$

$$Q = \frac{U_0 K}{4R} A_0 \sin(\phi_0) . \quad (6)$$

The amplitude A_{LIA} of the voltage u_d can be calculated by

$$A_{LIA} = 2\sqrt{I^2 + Q^2} = \frac{U_0 K}{2R} A_0 , \quad (7)$$

which enables a direct computation of the oscillation amplitude. The oscillation phase can directly be calculated by

$$\phi_{LIA} = \arctan\left(\frac{Q}{I}\right) = \phi_0 . \quad (8)$$

The lock-in amplifier enables a simultaneous amplitude and phase measurement of the cantilever oscillation which is insensitive to noise components outside the frequency range defined by the bandwidth of the low pass filters. However, in order to implement the multiplication with in-phase and quadrature sinusoidal signals on a digital signal processor (DSP), the sampling rate of the ADC needs to be 10 to 100 times higher than the oscillation frequency [29]. For micro-machined transducers with resonance frequencies of tens of MHz the required sampling rate can therefore exceed 100 MHz which leads to a high implementation complexity of the demodulator.

III. Proposed Demodulation

In this section, the proposed simplified demodulation method is described. In a first step, our previously presented demodulation method for determining the oscillation amplitude is presented [30]. Then, the method is extended to enable simultaneous amplitude and phase measurement.

A. In-Phase Demodulation

Figure 3 shows the previously presented method for a simplified demodulation of the oscillation amplitude. The bridge circuit is supplied by an AC-voltage with amplitude U_0, frequency ω_0 and an adjustable phase ϕ_c. The bridge circuit output voltage is applied to an instrumentation amplifier and the resulting output voltage $u_{d,AC}$ equals

$$u_{d,AC}(t) = \frac{U_0 K}{4R} A_0 \left[\cos(\phi_0 - \phi_c) - \cos(2\omega_0 t + \phi_0 + \phi_c)\right] . \quad (9)$$

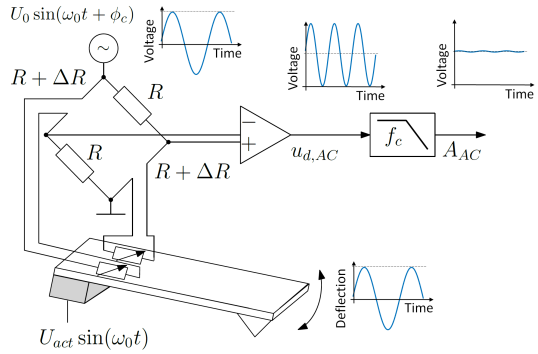

Fig. 3: In-phase demodulation. By supplying the bridge circuit with an electrical signal of the same frequency as the mechanical oscillation, the oscillation amplitude can directly be measured at the output of the bridge circuit [30].

Supplying the bridge circuit by an electrical signal of the same frequency ω_0 as the mechanical oscillation leads to a multiplication of the two electrical and mechanical oscillation. The instrumentation amplifier output voltage therefore contains a DC component proportional to the amplitude of the mechanical oscillation, as well as a component at frequency $2\omega_0$. The amplitude A_{AC} of the voltage $u_{d,AC}$ can be obtained after removing the $2\omega_0$ component by a low-pass filter with a $-3\,\mathrm{dB}$ bandwidth of f_c:

$$A_{AC} = \frac{U_0 K}{4R} A_0 \cos(\phi_0 - \phi_c) . \quad (10)$$

For a constant phase ϕ_0 the oscillation amplitude A_0 can therefore directly be obtained from (10). By comparing (10) with (7), it can be seen that the measurement of A_{AC} with the phase adjusted to $\phi_c = \phi_0$ corresponds to the upper branch of the lock-in amplifier demodulation, i.e. only the in-phase component of the oscillation is demodulated. Alternatively, if A_0 is constant and the phase is adjusted to $\phi_c = \phi_0 + \pi/2$, (10) enables a measurement of ϕ_0.

As pointed out in Section I, in many applications a simultaneous and independent measurement of oscillation amplitude and phase is required. However, if the oscillation amplitude is determined using (10), it is not possible to distinguish between a variation of amplitude and phase. The lack of a simultaneous amplitude and phase measurement is therefore a significant limitation of this method.

B. In-Phase and Quadrature Demodulation

Figure 4 shows the proposed demodulation method for simultaneous amplitude and phase measurement. The piezoresistive elements at the base of the cantilever are connected in two separate bridge circuits, which are supplied by in-phase ($\sin(\omega_0 t)$) and quadrature ($\cos(\omega_0 t)$) sinusoidal signals with amplitude U_0 and frequency ω_0. The piezoresistive elements experience the same variation (1) of their resistance. The bridge circuit output voltages are applied to two instrumenta-

Pre-print version of the article: M. Poik, D. Kohl, M. Mayr, C. Kerschner and G. Schitter, "A Mechatronic Lock-In Amplifier: Integrating Demodulation in Sensor Electronics for Measuring Mechanical Oscillations", *IEEE Transactions on Instrumentation and Measurement*, vol. 70, 2020. DOI: 10.1109/TIM.2020.3047208

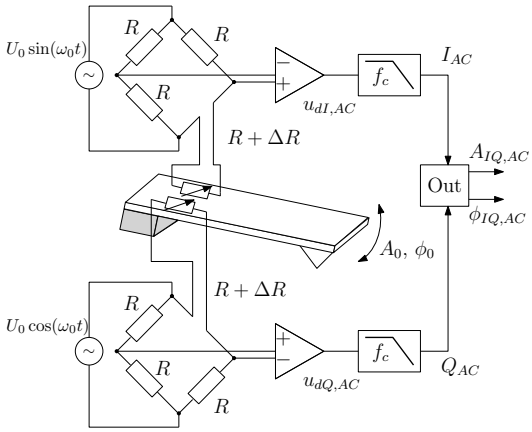

Fig. 4: Proposed in-phase and quadrature demodulation. Two piezoresistive elements at the base of the cantilever are connected in separate bridge circuits supplied with in-phase and quadrature sinusoidal signals. Amplitude and phase of the mechanical oscillation can be computed from the bridge circuit output voltages without external demodulator.

tion amplifiers with a gain G. Therefore, the resulting voltages $u_{dI,AC}$ and $u_{dQ,AC}$ equal

$$u_{dI,AC}(t) = \frac{U_0 K}{8R} A_0 \left[\cos(\phi_0) - \cos(2\omega_0 t + \phi_0)\right] , \quad (11)$$

$$u_{dQ,AC}(t) = \frac{U_0 K}{8R} A_0 \left[\sin(\phi_0) + \cos(2\omega_0 t + \phi_0)\right] . \quad (12)$$

Comparison of (11) and (12) with (3) and (4) shows that supplying the bridge circuits with in-phase and quadrature sinusoidal voltages leads to the same result as the multiplication with that voltages by a lock-in amplifier. After removing the $2\omega_0$ components by low-pass filters the voltages I_{AC} and Q_{AC} are obtained. The oscillation amplitude A_0 and phase ϕ_0 can therefore be determined in the same way as for the lock-in amplifier:

$$A_{IQ,AC} = 2\sqrt{I_{AC}^2 + Q_{AC}^2} = \frac{U_0 K}{4R} A_0 \quad (13)$$

$$\phi_{IQ,AC} = \arctan\left(\frac{Q_{AC}}{I_{AC}}\right) = \phi_0 . \quad (14)$$

Since the piezoresistive elements are now implemented in two quarter bridge circuits instead of a half bridge circuit, the sensitivity is reduced by a factor of 2. Another disadvantage of the quarter bridge circuits is that nonlinearities of the piezoresistive elements, as well as drift due to temperature variations are not compensated within the bridge circuit. However, by integrating 4 or 8 piezoresistive elements on the cantilever, two half bridge or full bridge circuits could be implemented to improve the sensitivity and to compensate for nonlinearities and temperature variations.

The connection of piezoresistive elements in two separate bridge circuits enables in-phase and quadrature demodulation and therefore a simultaneous measurement of amplitude and phase of the cantilever oscillation. The implementation requires no cumbersome external multiplications of electrical signals, and the low-pass filter could be easily integrated onto the chip. As in the lock-in amplifier, the computation of amplitude (13) and phase (14) is still required. However, the variation of the signals I_{AC} and Q_{AC} is defined by the low-pass filter bandwidth, as well as the speed of the amplitude variation defined by the measurement application, which is typically at least 10 to 100 times lower than the cantilever resonance frequency. Therefore the requirements for the digital implementation of the mathematical operations is significantly relaxed with respect to the demodulation by a lock-in amplifier.

IV. Experimental Implementation

Figure 5 shows a block diagram and photograph of the experimental setup. The self-sensing AFM cantilever and its connector can be seen in the top left image of Figure 5a. The connector is glued to a piezoelectric actuator which is connected to a function generator (Agilent 33500B, Santa Clara, US).

To implement the proposed method, the piezoresistive elements at the base of the cantilever have to be connected in two independent quarter bridge circuits. To this end, the electrical connections to the piezoresistive elements on the AFM chip (left circle in Figure 2) are opened by a focused ion beam, which allows the piezoresistive elements at the base of the cantilever (right circle in Figure 2) to be connected to two independent quarter bridge circuits implemented on an external PCB. The PCB is shown in the bottom image of Figure 5a with an annotation of the individual parts. The cantilever connector is inserted on the top of the PCB. Below the connector the two bridge circuits including trimmer resistors and capacitors for bridge circuit balancing (see Section IV-A) can be seen. They are supplied by in-phase ($U_0 \sin(\omega_0 t)$) and quadrature ($U_0 \cos(\omega_0 t)$) sinusoidal signals with an amplitude of $U_0 = 0.5\,\mathrm{V}$ and frequency ω_0, which are generated by a second function generator (Agilent 33500B, Santa Clara, US). The function generators are synchronized to ensure that the cantilever excitation frequency matches the frequency of the bridge supply voltages. The bridge supply voltages are applied via single-ended to differential converters to prevent any interaction between the two bridge circuits due to the common ground connection of the function generator. The bridge circuit output voltages are amplified by instrumentation amplifiers (AD8429) with a gain of 750. Offset compensation circuits for the instrumentation amplifiers are implemented as recommended in the datasheet, to eliminate any DC offset which would lead to a measurement error in the proposed method. The resulting voltages $u_{dI,AC}$ and $u_{dQ,AC}$ are applied to analog fourth-order low-pass filters with a crossover frequency of 500 Hz. The voltages I_{AC} and Q_{AC} are applied to an STM32F4 microcontroller operating at sampling rate of 1 kHz, which performs the mathematical operations (13) and (14) to obtain amplitude and phase of the cantilever oscillation.

For the implementation of the conventional method, the piezoresistive elements are configured in a half bridge circuit which is supplied by a DC voltage of $U_0 = 0.5\,\mathrm{V}$ and the output voltage u_d is amplified by an instrumentation amplifier (AD8429) with a gain of 750. The resulting voltage

Pre-print version of the article: M. Poik, D. Kohl, M. Mayr, C. Kerschner and G. Schitter, "A Mechatronic Lock-In Amplifier: Integrating Demodulation in Sensor Electronics for Measuring Mechanical Oscillations", *IEEE Transactions on Instrumentation and Measurement*, vol. 70, 2020. DOI: 10.1109/TIM.2020.3047208

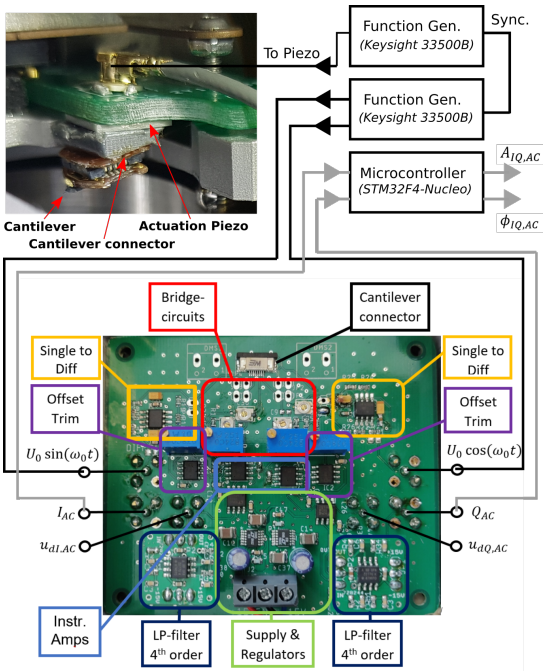

(a)

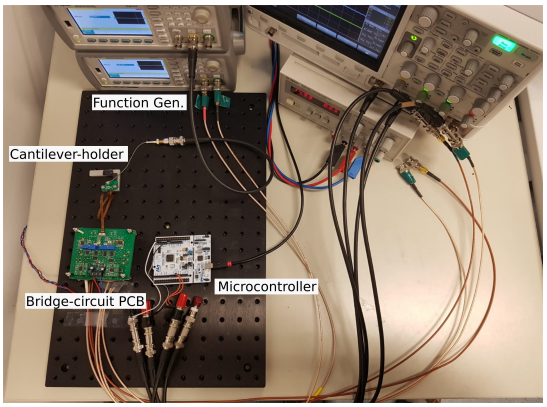

(b)

Fig. 5: (a) Block diagram of the experimental setup and close-up images of cantilever mount and PCB. (b) Photograph of the experimental setup.

is applied to a lock-in amplifier (Ametek 7270, Pennsylvania, US) with a selected fourth-order low-pass filter with a cross-over frequency of 500 Hz.

To verify the proposed method, the signals u_d, A_{LIA} and ϕ_{LIA} of the conventional method, as well as $u_{dI,AC}$, $A_{IQ,AC}$ and $\phi_{IQ,AC}$ of the proposed method, are recorded by an oscilloscope (Agilent DSO-X 2004A, Santa Clara, US).

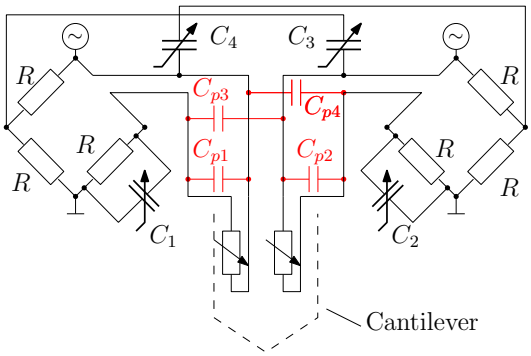

Fig. 6: Illustration of parasitic capacitances between the connectors of the piezoresistive elements on the cantilever. The bridge circuit imbalance due to C_{p1} and C_{p2} is compensated by the capacitors C_1 and C_2, and the crosstalk introduced by C_{p3} and C_{p4} is compensated by the capacitors C_3 and C_4, respectively.

A. Bridge circuit balancing and crosstalk compensation

If the proposed method is implemented using purely resistive bridge circuits as shown in Figure 4, a significant imbalance and cross-talk between the two bridge circuits can be observed. For instance, a bridge circuit which is balanced at DC, becomes unbalanced when operated at frequency ω_0. Additionally, a variation of the amplitude of the supply voltage in one bridge circuit leads to a change of the output voltage of the second bridge circuit.

The imbalance and cross-talk can be explained by parasitic capacitances between the closely spaced connections of the piezoresistive elements on the AFM chip. Since the bridge circuits are operated with AC voltages with a relatively high frequency of ω_0, parasitic capacitances in parallel to the piezoresistive elements and the resistors on the PCB can not be neglected. As illustrated in Figure 6, there are four parasitic capacitances (C_{p1} to C_{p4}) between the connectors of the piezoresistive elements. The capacitances C_{p1} and C_{p2} lead to the described imbalance when changing the operation frequency from DC to ω_0, while C_{p3} and C_{p4} lead to coupling and therefore a cross-talk between the two bridge circuits.

Adopting the approach proposed in [32], the influence of the parasitic capacitances can be compensated by integrating additional trimmer capacitors with a range of 8 pF to 40 pF, as shown in Figure 6. The capacitances C_1 and C_2 compensate for the imbalance due to C_{p1} and C_{p2}, while the capacitances C_3 and C_4 compensate for the cross-talk due to C_{p3} and C_{p4}. The compensation procedure is carried out prior to the demodulation and without cantilever oscillation. First, the two supply voltages with frequency ω_0 are subsequently turned on and the bridge circuits are balanced independently by manually adjusting the capacitances C_{p1} and C_{p2} such that the output voltages are nullified. Then, the cross-talk is removed by switching on both supply voltages simultaneously, and nullifying the output voltages of both bridge circuits by adjusting the capacitances C_{p3} and C_{p4}.

Pre-print version of the article: M. Poik, D. Kohl, M. Mayr, C. Kerschner and G. Schitter, "A Mechatronic Lock-In Amplifier: Integrating Demodulation in Sensor Electronics for Measuring Mechanical Oscillations", *IEEE Transactions on Instrumentation and Measurement*, vol. 70, 2020. DOI: 10.1109/TIM.2020.3047208

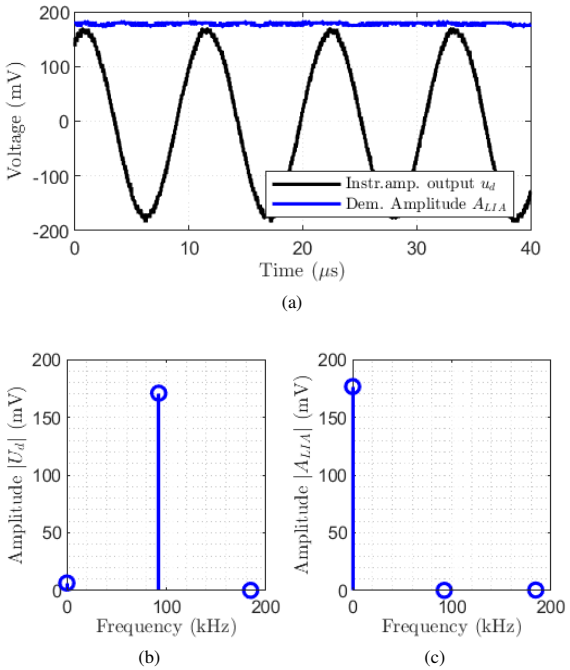

Fig. 7: Demodulation with Lock-In Amplifier: (a) Waveforms of the instrumentation amplifier output voltage u_d and the demodulated amplitude A_{LIA}. Spectral components of (b) u_d and (c) A_{LIA} at DC, ω_0 and $2\omega_0$.

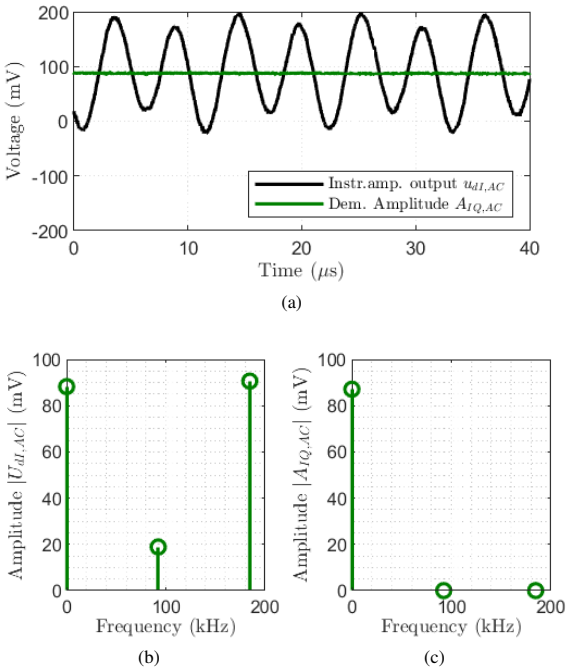

Fig. 8: Proposed demodulation: (a) Waveforms of the instrumentation amplifier output voltage $u_{dI,AC}$ and the demodulated amplitude $A_{IQ,AC}$. Spectral components of (b) $u_{dI,AC}$ and (c) $A_{IQ,AC}$ at DC, ω_0 and $2\omega_0$. The DC component of the instrumentation amplifier output voltage is proportional to the cantilever oscillation amplitude, which can therefore directly be obtained by low-pass filtering.

V. Experimental Results

To verify the working principle of the proposed demodulation method, the cantilever is excited at ω_0 by the piezoelectric actuator. The spectral components of the instrumentation amplifier output voltages and the demodulated amplitudes are analyzed to verify the equations derived in Section III.

Figure 7a shows the voltage u_d and the amplitude A_{LIA} for the demodulation by the lock-in amplifier. The corresponding spectral components of u_d and A_{LIA} at DC, ω_0 and $2\omega_0$ are shown in Figure 7b and Figure 7c, respectively. As expected from (2), u_d only shows a component at frequency ω_0. After demodulation by the lock-in amplifier the oscillation is converted to a DC value equal to the amplitude of u_d.

Figure 8a shows the voltage $u_{dI,AC}$ and the amplitude $A_{IQ,AC}$ obtained with the proposed demodulation method. Figure 8b and Figure 8c the corresponding spectral components at DC ω_0 and $2\omega_0$ are shown. The voltage $u_{dI,AC}$ in Figure 8a contains two main components at DC and $2\omega_0$, which is in accordance with (11). The oscillation amplitude can directly be obtained by low-pass filtering of $u_{dI,AC}$. The resulting DC voltage $A_{IQ,AC}$ in Figure 8a and Figure 8c is equal to $A_{LIA}/2$ (note the different scales of the vertical axes in Figure 7b-c and Figure 8b-c). The difference of a factor of 2 between $A_{IQ,AC}$ and A_{LIA} can be explained by the different sensitivities of the two demodulation methods (compare (7) and (13)).

The non-zero component of $u_{dI,AC}$ at ω_0, which can be seen in Figure 8b can be explained by an imperfect compensation of the parasitic capacitances. Due to the discrete implementation and the manual adjustment of the small capacitance values the bridge circuit compensation described in the previous section shows drift due to temperature variations. Any imbalance or cross-talk between the bridge circuits causes a feed-through of either the mechanical oscillation or the bridge supply voltage to the output, which leads to the spectral component at ω_0. It is expected that the compensation can be significantly improved by replacing the used capacitors with electrically adjustable capacitors, or by integrating compensation capacitors directly on the AFM chip, which is part of future work.

To demonstrate the capability to determine oscillation amplitude and phase by the proposed demodulation method, the amplitude and phase of the excitation voltage of the piezoelectric actuator is varied. Figure 9a shows the demodulated oscillation amplitudes A_{LIA} and $A_{IQ,AC}$ depending on the piezo excitation. The demodulated amplitudes are normalized by the measured oscillation at the maximum piezo excitation of 20 Vpp to eliminate the influence of different magnifications of the lock-in amplifier and the microcontroller output. The demodulation by the proposed method closely matches the results of the lock-in amplifier, which shows a linear depen-

Pre-print version of the article: M. Poik, D. Kohl, M. Mayr, C. Kerschner and G. Schitter, "A Mechatronic Lock-In Amplifier: Integrating Demodulation in Sensor Electronics for Measuring Mechanical Oscillations", *IEEE Transactions on Instrumentation and Measurement*, vol. 70, 2020. DOI: 10.1109/TIM.2020.3047208

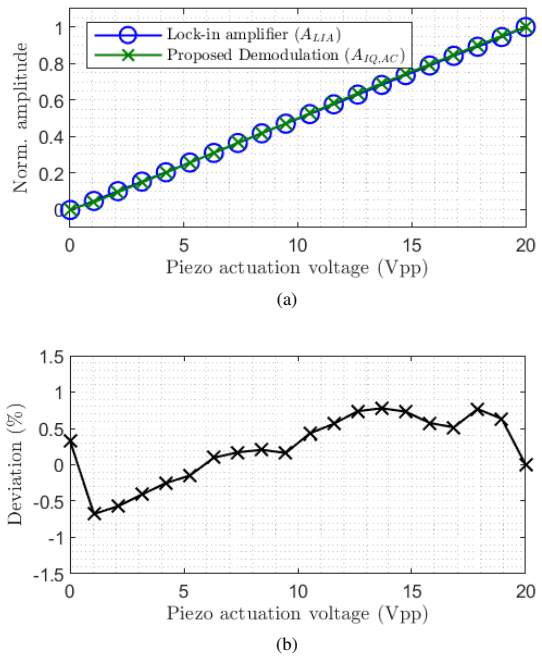

Fig. 9: (a) Comparison of the demodulated amplitudes A_{LIA} and $A_{IQ,AC}$, depending on the piezo voltage U_{act}. (b) Difference between $A_{IQ,AC}$ and A_{LIA}.

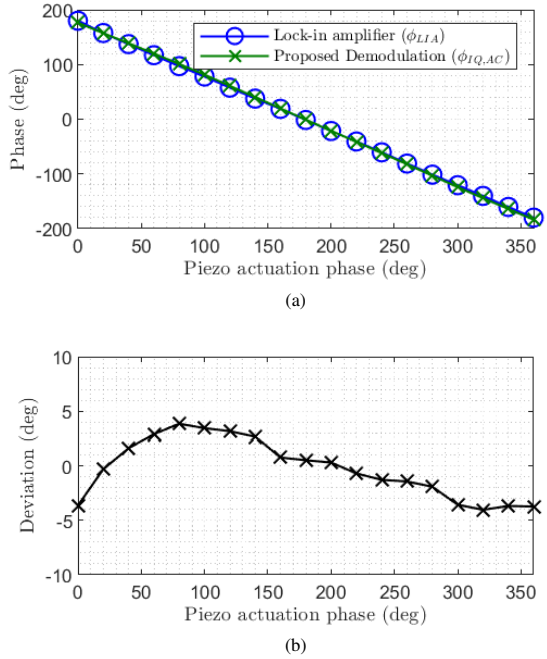

Fig. 10: (a) Comparison of the demodulated phases ϕ_{LIA} and $\phi_{IQ,AC}$, depending on the piezo phase. (b) Difference between $\phi_{IQ,AC}$ and ϕ_{LIA}.

dence between excitation amplitude and measured oscillation. Figure 9b shows the difference between the amplitude demodulation by the conventional and the proposed method. The deviation is $< 1\,\%$ for the entire range of piezo excitation voltages applicable by the used function generator.

In Figure 10a, the phase of the excitation voltage is varied and the resulting demodulated phases are shown. In order to enable a comparison between the proposed method and the lock-in amplifier, the reference phase of the lock-in amplifier is manually adjusted such that ϕ_{LIA} and $\phi_{IQ,AC}$ are equal at an excitation phase of $0°$. As expected, the demodulation by the proposed method closely matches the results of the lock-in amplifier, which is in accordance with (8) and (14). Figure 10b shows the difference between the phase demodulation by the conventional and the proposed method. The deviation is $< 5\,°$, which is $< 1.4\,\%$ of the total range of $360\,°$. The results show that the proposed method enables an accurate demodulation which can be implemented with low-cost off-the-shelf electronic components.

In summary, it has been shown that the proposed method omits the need for an external demodulator by integrating the lock-in technique in the sensor electronics, and thus enables a simplified measurement of amplitude and phase of mechanical oscillations.

VI. Conclusions

The presented demodulation method enables a simplified demodulation of the mechanical oscillations. It is analytically derived that the configuration of piezoresistive elements in AC bridge circuits which are operated at the mechanical oscillation frequency leads to a direct demodulation at the bridge output voltage. By connecting two piezoresistive elements in independent bridge circuits which are supplied with in-phase and quadrature sinusoidal signals, the proposed method enables a simultaneous measurement of amplitude and phase of the mechanical oscillation, thus integrating the lock-in technique in the sensor electronics. To verify the analytic analysis, the oscillation of an AFM cantilever with integrated piezoresistive elements is demodulated. The proposed method only requires low-pass filters which can easily be integrated on micro-machined oscillators and enables the development of cost-efficient and highly integrated sensors and transducers. The method is not limited to the detection of mechanical oscillations by piezoresistive sensors. For instance, the impedance variation of capacitive sensors could be demodulated by configuring the capacitances in AC bridge circuits in a similar way. Ongoing work is focused on the integration and application of the method in resonant MEMS mirrors and cantilever-based resonant sensors.

Acknowledgment

The separation of the piezoresistive elements on the AFM chip by a focused ion beam was carried out using facilities at the University Service Centre for Transmission Electron Microscopy, Vienna University of Technology, Austria.

Pre-print version of the article: M. Poik, D. Kohl, M. Mayr, C. Kerschner and G. Schitter, "A Mechatronic Lock-In Amplifier: Integrating Demodulation in Sensor Electronics for Measuring Mechanical Oscillations", *IEEE Transactions on Instrumentation and Measurement*, vol. 70, 2020. DOI: 10.1109/TIM.2020.3047208

References

[1] R. Schroedter, M. Schwarzenberg, A. Dreyhaupt, R. Barth, T. Sandner, and K. Janschek, "Microcontroller based closed-loop control of a 2D quasi-static/resonant microscanner with on-chip piezo-resistive sensor feedback," *MOEMS and Miniaturized Systems XVI*, vol. 10116, p. 1011605, 2017.

[2] L. Fu, A. Jain, H. Xie, C. Cranfield, and M. Gu, "Nonlinear optical endoscopy based on a double-clad photonic crystal fiber and a MEMS mirror," *Optics Express*, vol. 14, no. 3, pp. 1027–1032, 2006.

[3] Z. Qiu and W. Piyawattanametha, "MEMS actuators for optical microendoscopy," *Micromachines*, vol. 10, no. 2, p. 85, 2019.

[4] R. Raiteri, M. Grattarola, H.-J. Butt, and P. Skladal, "Micromechanical cantilever-based biosensors," *Sensors and Actuators B: Chemical*, vol. 79, pp. 115–126, 2001.

[5] P. S. Waggoner and H. G. Craighead, "Micro- and nanomechanical sensors for environmental, chemical, and biological detection," *Lab on a Chip*, vol. 7, no. 10, pp. 1238–1255, 2007.

[6] R. García and R. Pérez, "Dynamic atomic force microscopy methods," *Surface Science Reports*, vol. 47, no. 6-8, pp. 197–301, 2002.

[7] H. W. Yoo, N. Druml, D. Brunner, C. Schwarzl, T. Thurner, M. Hennecke, and G. Schitter, "MEMS-based lidar for autonomous driving," *Elektrotechnik und Informationstechnik*, vol. 135, no. 6, pp. 408–415, 2018. [Online]. Available: http://dx.doi.org/10.1007/s00502-018-0635-2

[8] A. San Paulo and R. García, "Tip-surface forces, amplitude, and energy dissipation in amplitude-modulation (tapping mode) force microscopy," *Physical Review B - Condensed Matter and Materials Physics*, vol. 64, no. 19, pp. 1 934 111–1 934 114, 2001.

[9] N. V. Lavrik, M. J. Sepaniak, and P. G. Datskos, "Cantilever transducers as a platform for chemical and biological sensors," *Review of Scientific Instruments*, vol. 75, no. 7, pp. 2229–2253, 2004.

[10] B. N. Johnson and R. Mutharasan, "Biosensing using dynamic-mode cantilever sensors: A review," *Biosensors and Bioelectronics*, vol. 32, no. 1, pp. 1–18, 2012.

[11] G. De Simoni, G. Signore, M. Agostini, F. Beltram, and V. Piazza, "A surface-acoustic-wave-based cantilever bio-sensor," *Biosensors and Bioelectronics*, vol. 68, pp. 570–576, 2015.

[12] J. Park, S. Nishida, P. Lambert, H. Kawakatsu, and H. Fujita, "High-resolution cantilever biosensor resonating at air-liquid in a microchannel," *Lab on a Chip*, vol. 11, no. 24, pp. 4187–4193, 2011.

[13] Y. Martin, C. C. Williams, and H. K. Wickramasinghe, "Atomic force microscope-force mapping and profiling on a sub 100-Å scale," *Journal of Applied Physics*, vol. 61, no. 10, pp. 4723–4729, 1987.

[14] T. R. Albrecht and C. F. Quate, "Atomic resolution imaging of a nonconductor by atomic force microscopy," *Journal of Applied Physics*, vol. 62, no. 7, pp. 2599–2602, 1987.

[15] T. Fukuma, J. I. Kilpatrick, and S. P. Jarvis, "Phase modulation atomic force microscope with true atomic resolution," *Review of Scientific Instruments*, vol. 77, no. 123703, 2006.

[16] D. Raghavan, X. Gu, T. Nguyen, M. VanLandingham, and A. Karim, "Mapping polymer heterogeneity using atomic force microscopy phase imaging and nanoscale indentation," *Macromolecules*, vol. 33, no. 7, pp. 2573–2583, 2000.

[17] K. M. Goeders, J. S. Colton, and L. A. Bottomley, "Microcantilevers: Sensing chemical interactions via mechanical motion," *Chemical Reviews*, vol. 108, no. 2, pp. 522–542, 2008.

[18] S. Alexander, L. Hellemans, M. O., J. Schneir, V. Elings, P. K. Hansma, M. Longmire, and J. Gurley, "An atomic-resolution atomic-force microscope implemented using an optical lever," *Journal of Applied Physics*, vol. 65, no. July 1988, pp. 164–167, 1989.

[19] L. Gammelgaard, P. A. Rasmussen, M. Calleja, P. Vettiger, and A. Boisen, "Microfabricated photoplastic cantilever with integrated photoplastic/carbon based piezoresistive strain sensor," *Applied Physics Letters*, vol. 88, no. 11, 2006.

[20] C. L. Britton, R. L. Jones, P. I. Oden, Z. Hu, R. J. Warmack, S. F. Smith, W. L. Bryan, and J. M. Rochelle, "Multiple-input microcantilever sensors," *Ultramicroscopy*, vol. 82, no. 1-4, pp. 17–21, 2000.

[21] L. G. Carrascosa, M. Moreno, M. Álvarez, and L. M. Lechuga, "Nanomechanical biosensors: A new sensing tool," *TrAC - Trends in Analytical Chemistry*, vol. 25, no. 3, pp. 196–206, 2006.

[22] S. C. Minne, S. R. Manalis, and C. F. Quate, "Parallel atomic force microscopy using cantilevers with integrated piezoresistive sensors and integrated piezoelectric actuators," *Applied Physics Letters*, vol. 67, no. 26, pp. 3918–3920, 1995.

[23] G. Yoshikawa, H. P. Lang, T. Akiyama, L. Aeschimann, U. Staufer, P. Vettiger, M. Aono, T. Sakurai, and C. Gerber, "Sub-ppm detection of vapors using piezoresistive microcantilever array sensors," *Nanotechnology*, vol. 20, no. 1, p. 015501, 2009.

[24] T. Ando, N. Kodera, E. Takai, D. Maruyama, K. Saito, and A. Toda, "A High-speed Atomic Force Microscope for Studying Biological Macromolecules," *Proceedings of the National Academy of Sciences*, vol. 98, no. 22, pp. 12 468–12 472, 2001.

[25] T. Ando, T. Uchihashi, and T. Fukuma, "High-speed atomic force microscopy for nano-visualization of dynamic biomolecular processes," *Progress in Surface Science*, vol. 83, no. 7-9, pp. 337–437, 2008.

[26] M. O. Sonnaillon, R. Urteaga, and F. J. Bonetto, "High-frequency digital lock-in amplifier using random sampling," *IEEE Transactions on Instrumentation and Measurement*, vol. 57, no. 3, pp. 616–621, 2008.

[27] M. Ayat, M. A. Karami, S. Mirzakuchaki, and A. Beheshti-Shirazi, "Design of Multiple Modulated Frequency Lock-In Amplifier for Tapping-Mode Atomic Force Microscopy Systems," *IEEE Transactions on Instrumentation and Measurement*, vol. 65, no. 10, pp. 2284–2292, 2016.

[28] J. D. Adams, G. Parrott, C. Bauer, T. Sant, L. Manning, M. Jones, B. Rogers, D. McCorkle, and T. L. Ferrell, "Nanowatt chemical vapor detection with a self-sensing, piezoelectric microcantilever array," *Applied Physics Letters*, vol. 83, no. 16, pp. 3428–3430, 2003.

[29] M. G. Ruppert, D. M. Harcombe, M. R. Ragazzon, S. O. Reza Moheimani, and A. J. Fleming, "A review of demodulation techniques for amplitude-modulation atomic force microscopy," *Beilstein Journal of Nanotechnology*, vol. 8, no. 1, pp. 1407–1426, 2017.

[30] M. Poik, D. Kohl, M. Mayr, C. Kerschner, and G. Schitter, "Efficient Demodulation for Measuring the Amplitude of Mechanical Oscillations," in *2020 IEEE International Instrumentation and Measurement Technology Conference (I2MTC)*. IEEE, 2020, pp. 1–5.

[31] M. G. Ruppert and Y. K. Yong, "Design of Hybrid Piezoelectric / Piezoresistive Cantilevers for Dynamic-mode Atomic Force Microscopy," in *Proceedings of the 2018 IEEE/ASME International Conference on Advanced Intelligent Mechatronics (AIM)*. IEEE, 2018, pp. 144–149.

[32] S. Kuiper and G. Schitter, "MIMO self-sensing control of a piezoelectric tube scanner," in *Proceedings of the ASME 2009 Dynamic Systems and Control Conference, Hollywood, CA, USA*, 2009, pp. 811–817.

Pre-print version of the article: M. Poik, D. Kohl, M. Mayr, C. Kerschner and G. Schitter, "A Mechatronic Lock-In Amplifier: Integrating Demodulation in Sensor Electronics for Measuring Mechanical Oscillations", *IEEE Transactions on Instrumentation and Measurement*, vol. 70, 2020. DOI: 10.1109/TIM.2020.3047208